



Published in final edited form as:

Nat Struct Mol Biol. 2008 May ; 15(5): 485–493. doi:10.1038/nsmb.1412.

## Sequence-directed DNA export guides chromosome translocation during sporulation in *Bacillus subtilis*

Jerod L Ptacin<sup>1,7</sup>, Marcelo Nollmann<sup>1,7</sup>, Eric C Becker<sup>2</sup>, Nicholas R Cozzarelli<sup>1,6</sup>, Kit Pogliano<sup>2</sup>, and Carlos Bustamante<sup>3,4,5</sup>

<sup>1</sup> Department of Molecular and Cell Biology, 642 Stanley Hall, University of California, Berkeley, California 94720, USA

<sup>2</sup> Division of Biological Sciences, 4114 Natural Sciences Building, University of California, San Diego, California 92093, USA

<sup>3</sup> Department of Physics, 231 Birge Hall, University of California, Berkeley, California 94720, USA

<sup>4</sup> Howard Hughes Medical Institute, USA

<sup>5</sup> Lawrence Berkeley National Laboratory, 1 Cyclotron Road, Berkeley, California, 94720, USA

### Abstract

In prokaryotes, the transfer of DNA between cellular compartments is essential for the segregation and exchange of genetic material. SpoIIIE and FtsK are AAA+ ATPases responsible for intercompartmental chromosome translocation in bacteria. Despite functional and sequence similarities, these motors were proposed to use drastically different mechanisms: SpoIIIE was suggested to be a unidirectional DNA transporter that exports DNA from the compartment in which it assembles, whereas FtsK was shown to establish translocation directionality by interacting with highly skewed chromosomal sequences. Here we use a combination of single-molecule, bioinformatics and *in vivo* fluorescence methodologies to study the properties of DNA translocation by SpoIIIE *in vitro* and *in vivo*. These data allow us to propose a sequence-directed DNA exporter model that reconciles previously proposed models for SpoIIIE and FtsK, constituting a unified model for directional DNA transport by the SpoIIIE/FtsK family of AAA+ ring ATPases.

The segregation and exchange of genetic material are central to the processes of cell division and evolution. Although mechanisms of genetic transfer between cellular compartments are diverse, all require the movement of DNA across cellular membranes. A dramatic example of intercellular transmembrane DNA transport is the segregation of chromosomes during sporulation in *Bacillus subtilis*. During this process, newly replicated chromosomes are rearranged into an elongated structure, or axial filament, in which the origin of replication of each chromosome is tethered to opposite cell poles<sup>1,2</sup>. Next, the division plane is relocated to one pole, creating two asymmetric cellular compartments (the forespore and the mother cell) and trapping the origin-proximal 30% of one chromosome within the forespore<sup>3,4</sup>. The septally

Correspondence should be addressed to C.B. (carlos@alice.berkeley.edu).

<sup>6</sup>Deceased.

<sup>7</sup>These authors contributed equally to this work.

Note: Supplementary information is available on the Nature Structural & Molecular Biology website.

#### AUTHOR CONTRIBUTIONS

J.L.P. and M.N. planned, collected and interpreted single-molecule, biochemical and fluorescence data; E.C.B. performed time-lapse fluorescence studies of SpoIIIE-SK chimera and compartment-specific GFP-tagging experiments; J.L.P., M.N., E.C.B., K.P. and C.B. wrote the paper.

Reprints and permissions information is available online at <http://npg.nature.com/reprintsandpermissions>

bound DNA translocase SpoIIIE assembles on the trapped chromosome and uses the energy of ATP hydrolysis to rapidly transfer the remaining ~3 megabases (Mb) of DNA from the mother cell into the forespore<sup>5-7</sup>. Genetic evidence suggests that SpoIIIE also functions during vegetative growth to clear DNA from division septa<sup>8-10</sup>. Both functions require that SpoIIIE mobilize DNA directionally.

FtsK, a closely related DNA translocase from *Escherichia coli*, is involved in the coordination of chromosome segregation and cell division<sup>11,12</sup>. FtsK brings the sites of chromosome dimer resolution (*dif* sites) into close proximity by translocating DNA directionally<sup>13</sup>. SpoIIIE and FtsK are composed of an N-terminal transmembrane domain involved in septal localization<sup>14-16</sup>, a putatively unstructured linker and a C-terminal motor domain involved in DNA translocation (Fig. 1a), which itself is composed of three separate subdomains:  $\alpha$ ,  $\beta$  and  $\gamma$ <sup>7,16,17</sup>. Genetic and single-molecule studies showed that the translocation directionality of FtsK is dictated by specific chromosomal DNA sequence motifs GGGNAGGG (FtsK orienting polar sequence, KOPS)<sup>18</sup> or GNGNAGGG (FtsK recognition sequence, FRS)<sup>19</sup>. The interaction of FtsK with KOPS is orientation specific: when encountering KOPS from the 3' end of the G-rich strand (nonpermissive direction) FtsK pauses and frequently reverses its translocation direction, but it passes unobstructed when encountering KOPS from the opposite direction (permissive orientation)<sup>18-20</sup> (Fig. 1b, left). The KOPS distribution is highly skewed (defined as the percentage of occurrences of the sequence on the leading versus the lagging strand of DNA replication) in the *E. coli* chromosome and switches strand and orientation at *dif* (Fig. 1b, right). Thus, this orientation-specific recognition mechanism and the asymmetric chromosomal distribution of KOPS direct FtsK translocation toward *dif* from any location along the chromosome.

The high sequence homology and similar functions of FtsK and SpoIIIE imply a common translocation mechanism. However, fluorescence microscopy studies suggested that SpoIIIE is a unidirectional DNA transporter that exports DNA out of the compartment in which it is expressed<sup>21</sup> (the unidirectional exporter model, shown in Figure 1c). This model proposed that the directionality of DNA export is regulated by the asymmetric partitioning and cell-specific assembly of SpoIIIE<sup>21,22</sup>. The fact that SpoIIIE is expressed throughout vegetative growth implied the existence of another unidentified factor that regulates translocation polarity in the absence of cellular asymmetry<sup>21,22</sup>. Recent work showed that, in a *racA soj-spo0J* mutant background, the misorientation of the chromosome relative to the septum caused SpoIIIE to translocate the chromosome out of the forespore<sup>23</sup>. This result suggests that SpoIIIE directional DNA transfer may also be regulated by the polarity of the chromosome itself. However, there is no direct evidence for a DNA sequence-directed mechanism for SpoIIIE translocation directionality. To clarify these conflicting models, we used single-molecule, bioinformatics and fluorescence microscopy methods to demonstrate that specific interactions between the  $\gamma$ -domain of SpoIIIE and specific, highly skewed chromosomal DNA sequences (SpoIIIE recognition sequence or SRS) regulate the compartment-specific activation of a mother-cell SpoIIIE complex responsible for DNA export into the forespore. This sequence-directed DNA exporter model unifies conflicting sequence-directed and exporter models and explains the establishment of directional DNA translocation by the FtsK/SpoIIIE family of DNA translocases.

## RESULTS

### DNA translocation by SpoIIIE<sub>C</sub> does not require SpoIIIE- $\gamma$

Previous measurements of DNA translocation by SpoIIIE have relied on indirect bulk methods or static microscopy<sup>6,7</sup>. Here, we used a simplified *in vitro* system to observe directly the dynamics of DNA translocation by single SpoIIIE motors using magnetic tweezers. A single nicked DNA molecule is tethered between a magnetic particle and a glass surface, and DNA

translocation by the soluble C-terminal motor domain of SpoIII<sup>E</sup><sub>7</sub> (SpoIII<sup>E</sup><sub>C</sub>; Fig. 1a) is monitored by the shortening of the DNA extension due to the formation of a DNA loop (Supplementary Fig. 1a and Supplementary Methods online). In these experiments, SpoIII<sup>E</sup><sub>C</sub> translocated DNA rapidly and processively at rates of  $4 \pm 1 \text{ kb s}^{-1}$  (Supplementary Fig. 1b,d), notably faster than estimated translocation velocities *in vivo* ( $\sim 1.5 \text{ kb s}^{-1}$  per chromosomal arm)<sup>24–26</sup>. This difference could be due to protein or DNA roadblocks, or larger loads opposing translocation *in vivo*. Recent findings showed that FtsK- $\gamma$  is required for KOPS recognition<sup>27,28</sup>. On the basis of the sequence similarity between FtsK- $\gamma$  and SpoIII<sup>E</sup>- $\gamma$ , we predicted that SpoIII<sup>E</sup>- $\gamma$  may be involved in regulating the directionality of DNA transfer during sporulation but not in the mechanical process of DNA translocation itself. To test these predictions, we first examined the *in vitro* motor properties of SpoIII<sup>E</sup><sub>C</sub>- $\Delta\gamma$ , a truncation mutant of SpoIII<sup>E</sup><sub>C</sub> lacking the  $\gamma$ -domain (Supplementary Methods). SpoIII<sup>E</sup><sub>C</sub>- $\Delta\gamma$  was able to translocate DNA at rates that were only slightly slower than SpoIII<sup>E</sup><sub>C</sub> ( $3 \pm 1 \text{ kb s}^{-1}$ ; Supplementary Fig. 1c,e), showing that SpoIII<sup>E</sup>- $\gamma$  is not essential for the motor activity of SpoIII<sup>E</sup> *in vitro*.

### SpoIII<sup>E</sup>- $\gamma$ is required for directional DNA translocation *in vivo*

We investigated the role of SpoIII<sup>E</sup>- $\gamma$  *in vivo* during sporulation by testing the ability of SpoIII<sup>E</sup>- $\Delta\gamma$  to rescue a *spoIII<sup>E</sup>*-null strain and produce viable spores (Methods). The genes encoding wild-type SpoIII<sup>E</sup> or SpoIII<sup>E</sup>- $\Delta\gamma$  under control of the *spoIII<sup>E</sup>* promoter were integrated into *spoIII<sup>E</sup>*-null strains (hereafter referred to as SpoIII<sup>E</sup><sup>★</sup> and SpoIII<sup>E</sup><sup>★</sup>- $\Delta\gamma$ , respectively; Supplementary Methods). The ability of the SpoIII<sup>E</sup><sup>★</sup> strain to produce viable spores was similar to that of a wild-type strain<sup>21</sup>, but the SpoIII<sup>E</sup><sup>★</sup>- $\Delta\gamma$  strain produced 10,000-fold fewer viable spores than SpoIII<sup>E</sup><sup>★</sup> (Fig. 2a and Supplementary Table 1 online). Thus, SpoIII<sup>E</sup>- $\gamma$  is not necessary for DNA translocation *in vitro* but is necessary for efficient sporulation *in vivo*.

To understand this sporulation defect triggered by the lack of SpoIII<sup>E</sup>- $\gamma$ , we used a time-lapse fluorescence microscopy technique<sup>23</sup> to characterize quantitatively the dynamics of chromosome translocation *in vivo* by SpoIII<sup>E</sup>. Synchronized sporulating cultures were grown on agar pads and imaged at regular intervals by fluorescence microscopy. To measure DNA translocation velocities and to observe the behavior of various SpoIII<sup>E</sup> mutants *in vivo*, we quantified the fluorescence intensity of DNA in the forespore versus total fluorescence intensity in the cell at different time points during sporulation (Supplementary Methods). Wild-type *B. subtilis* and SpoIII<sup>E</sup><sup>★</sup> strains translocated DNA exclusively from the mother cell to the forespore ( $n = 243$ ; Fig. 2b,c and Supplementary Video 1 online) at velocities of  $500 \pm 80 \text{ bp s}^{-1}$  per chromosomal arm. The slightly slower DNA translocation velocity in these experiments versus previous estimates may be attributed to differences in our experimental conditions, such as temperature ( $30^\circ\text{C}$  versus  $37^\circ\text{C}$ ) and the presence of intercalated fluorescent dyes (Methods) that could affect SpoIII<sup>E</sup> velocities *in vivo*.

In contrast, SpoIII<sup>E</sup><sup>★</sup>- $\Delta\gamma$  cells showed a marked defect in directional chromosome transfer, as at least 40% of the cells were observed to reverse-translocate DNA out of the forespore, and none completed forward chromosome translocation ( $n = 349$ ; Supplementary Video 2 online). Quantitative analysis of these events revealed a frequent DNA translocation defect in which forward translocation was followed by a pause and a subsequent reversal of the translocation direction out of the forespore (Fig. 2b,d and Supplementary Fig. 2a–d online). The mean distance translocated by SpoIII<sup>E</sup>- $\Delta\gamma$  before pausing was  $0.75 \pm 0.3 \text{ Mb}$  per chromosome arm, and the mean pause length was  $20 \pm 10 \text{ min}$  (Supplementary Fig. 3b,c online). The velocities of forward and reverse DNA translocation in these events were indistinguishable (Fig. 2e) and consistently  $\sim 25\%$  slower than in wild-type and SpoIII<sup>E</sup><sup>★</sup> strains ( $n = 77$ ,  $P$ -value = 0.0001; Fig. 2e), mimicking the difference in translocation rates measured in single-molecule *in*

*in vitro* experiments between SpoIII<sub>E</sub>C and SpoIII<sub>E</sub>C-Δγ (Supplementary Fig. 1). A control strain expressing only SpoIII<sub>E</sub>36, an ATPase mutant of SpoIII<sub>E</sub><sup>5</sup>, did not show any forward or reverse translocation (data not shown). Previous studies showed that FtsK-γ is necessary for sequence recognition *in vitro*<sup>27,28</sup> and *in vivo* in a plasmid resolution assay<sup>28</sup>. Our data show that the SpoIII<sub>E</sub>-γ is necessary for regulating the directionality of chromosomal transport *in vivo*. In particular, the frequent *in vivo* translocation direction reversals observed in the SpoIII<sub>E</sub><sup>\*</sup>-Δγ strain show that the translocation directionality imparted by SpoIII<sub>E</sub> is not simply due to its partitioning to the mother cell before septation (Fig. 1c) and suggest that the substrate polarity is also involved in maintaining the directionality of transfer. The long pause durations required for reversing translocation direction *in vivo* (~20 min) suggest that the mechanism responsible for translocation reversal is slow, possibly involving the recruitment of SpoIII<sub>E</sub> and the assembly of the forespore complex. This observation, together with the high processivity of SpoIII<sub>E</sub>-Δγ *in vivo*, is also inconsistent with a strictly sequence-directed model (Fig. 1b).

### Identification and characterization of SRS

The role of SpoIII<sub>E</sub>-γ in regulating directional DNA transfer and the function of FtsK-γ in KOPS recognition<sup>27,28</sup> raised the possibility that orientation-specific interactions between SpoIII<sub>E</sub> and highly skewed SRS sequences could control directional DNA transfer during sporulation (Fig. 3a; Supplementary Fig. 3a and Supplementary Methods). Sequence similarity between FtsK-γ and SpoIII<sub>E</sub>-γ, and the high skew of KOPS along the chromosome of *B. subtilis* (84%,  $P$ -value =  $1 \times 10^{-27}$ ), suggested that KOPS may guide directional translocation by SpoIII<sub>E</sub>. To test the effect of KOPS on SpoIII<sub>E</sub> DNA translocation, we used an *in vitro* magnetic tweezers assay for sequence recognition (Fig. 3b and Methods) that was previously used to detect specific KOPS-FtsK interactions<sup>18,27,29</sup>. In this assay, we quantified the recognition probability of a triple tandem repeat of KOPS (3 × KOPS, or 3 × SRS1) by measuring the reversal frequency of SpoIII<sub>E</sub>C at DNA extensions corresponding to the location of the test sequence on the molecule (Supplementary Methods). Previous studies determined that FtsK recognizes KOPS with a probability of ~40%<sup>19</sup>. Notably, we found that SpoIII<sub>E</sub>C recognizes KOPS with a probability of only  $3 \pm 3\%$  per sequence (Supplementary Table 2 online), showing that at least this instance of KOPS cannot guide SpoIII<sub>E</sub> during sporulation.

To identify other candidate SRS sequences, we conducted a bio-informatics search for highly skewed octameric DNA sequences in the *B. subtilis* chromosome that switched strand at *dif* (Supplementary Table 2, Supplementary Fig. 4 and Supplementary Methods online). The role of SpoIII<sub>E</sub> in vegetative growth<sup>10</sup> and the location of *dif* at the center of the terminus of replication in *B. subtilis*<sup>30,31</sup> suggest that the *dif* region is the last chromosomal fragment to be translocated into the forespore during sporulation. We tested six candidate sequences identified with this approach (SRS1–6) using the magnetic tweezers assay for specific DNA sequence recognition. We observed similar low levels of recognition (~5% per SRS instance) for SRS1–5, despite their high chromosomal skews and low  $P$ -values (that is, the probability that their asymmetric chromosomal distributions occurred by chance; see Supplementary Fig. 5a and Supplementary Table 2 online). Notably, on DNA molecules containing 3 × SRS6 (GAGAAGGG), SpoIII<sub>E</sub>C frequently paused and reversed at DNA extensions corresponding to the SRS6 repeats with a frequency of  $29 \pm 5\%$  per instance (Fig. 3c; Supplementary Table 2). However, to guarantee directional DNA movement, SpoIII<sub>E</sub> must be able to recognize SRS6 in an orientation-specific manner. We implemented a DNA triplex-displacement assay in which orientation specificity is detected by differences in triplex-displacement rates by SpoIII<sub>E</sub>C on DNA substrates containing permissive or nonpermissive SRS<sup>19</sup> (Fig. 3d). Consistent with the lack of KOPS recognition, triplex-displacement rates by SpoIII<sub>E</sub>C were similar on substrates containing 3 × SRS1 (KOPS) in permissive or nonpermissive orientations (Supplementary Fig. 5b). In contrast, displacement rates on substrates containing SRS6 showed

a considerable difference ( $2.5 \pm 0.5$ -fold) between permissive and nonpermissive orientations (Fig. 3e).

This robust and orientation-specific recognition of SRS6 *in vitro* prompted us to examine its relevance *in vivo* by using a genetic assay for sequence recognition (Supplementary Figs. 6a,b and Supplementary Methods online). This assay relies on a kinetic competition between SpoIIIE translocation and the Cre-mediated recombination of a chromosomal kanamycin-resistance cassette flanked by *loxP*<sup>32</sup>. Recognition of a tandem repeat of SRS6 that disrupts forward translocation by SpoIIIE increases the frequency of recombination of the kanamycin-resistance gene in the mother cell, and thus the frequency of kanamycin-sensitive spores. Using this assay, we measured an 8% increase in kanamycin-sensitive spores in the nonpermissive versus the permissive SRS6 strain ( $n = 24$ ,  $P$ -value = 0.02), suggesting that SpoIIIE recognizes SRS6 specifically *in vivo* during sporulation.

SRS6 is a member of AIMS (architecture imparting sequences)<sup>33</sup>. On the *B. subtilis* chromosome, SRS6 is highly skewed (81%,  $P$ -value =  $1 \times 10^{-15}$ ) and switches strand at *dif*. Surprisingly, SRS6 does not switch at *oriC* but at a locus approximately 250 kb to the left of *oriC* (Fig. 3a,f). Interestingly, this is the location of the polar localization region (PLR), the centromere-like sequence in *B. subtilis* (extending from -150 kb to -300 kb) required to segregate the *oriC* region to the cell pole during sporulation<sup>34</sup>. It is likely that SRS6 is an instance of a degenerate sequence family or motif, such as that represented by KOPS<sup>19,29</sup>. In a preliminary search for a consensus SRS, we found that GAG(C/A)AGGG is the most likely SRS motif (Supplementary Results and Supplementary Table 3 online). This putative family of sequences has a skew of 82%, a significantly higher density and thus a lower  $P$ -value ( $1 \times 10^{-26}$ ) than SRS6.

### SpoIIIE- $\gamma$ recognizes SRS6 specifically *in vitro* and *in vivo*

The orientation-specific recognition of SRS6 by SpoIIIE and the requirement of SpoIIIE- $\gamma$  for directional DNA transfer *in vivo* suggest that SpoIIIE- $\gamma$  specifically mediates SRS6 interactions. To test this prediction, we introduced a single mutation in the putative DNA binding region of SpoIIIE- $\gamma$  (SpoIIIE<sub>C</sub>-R773A)<sup>28</sup> and measured the ability of this protein to recognize SRS6 *in vitro* and to support sporulation *in vivo*. In the magnetic tweezers assay, SRS6 recognition by SpoIIIE<sub>C</sub>-R773A was reduced by approximately two-fold (Supplementary Fig. 5c and Supplementary Table 2). Consistent with this reduction, SpoIIIE<sup>\*</sup>-R773A produced three-fold fewer viable spores than SpoIIIE<sup>\*</sup> (Supplementary Table 1), indicating that SpoIIIE- $\gamma$  mediates direct interactions with SRS6 *in vivo*. This modest defect in spore titers *in vivo* agrees with calculations that predicted that large changes in sequence-recognition probability produce minor changes in the efficiency of directional DNA translocation<sup>19</sup>.

### FtsK- $\gamma$ and SpoIIIE- $\gamma$ are exchangeable modules

The sequence-directed model for DNA translocation directionality predicts that SpoIIIE- $\gamma$ -SRS6 interactions are modular. Thus, the exchange of SpoIIIE- $\gamma$  by FtsK- $\gamma$  should switch the recognition specificity of SpoIIIE from SRS to KOPS. We tested this prediction by replacing SpoIIIE- $\gamma$  with FtsK- $\gamma$  to create a chimera termed SpoIIIE<sub>C</sub>-SK (Fig. 4a), and assayed its interaction with KOPS using the magnetic tweezers and triplex-displacement assays. In magnetic tweezers experiments, SpoIIIE<sub>C</sub>-SK reversed at DNA extensions corresponding to the location of  $3 \times$  KOPS with a probability of ~35% per KOPS instance (Fig. 4b, Supplementary Fig. 5e and Supplementary Table 2) and showed a pattern of sequence recognition similar to that of FtsK<sub>50C27</sub>. Recognition of KOPS by SpoIIIE<sub>C</sub>-SK is orientation specific, as triplex-displacement rates on permissive  $3 \times$  KOPS substrates were  $1.8 \pm 0.25$ -fold faster than on nonpermissive substrates (Fig. 4c). Notably, the turnaround probability of



SpoIII<sub>C</sub>-SK at SRS6 was only 3% (Supplementary Figs. 2 and 5d), indicating that SpoIII<sub>C</sub>-SK can recognize KOPS but not SRS *in vitro*.

The efficient, orientation-specific KOPS recognition by SpoIII<sub>C</sub>-SK *in vitro* and the high skew of KOPS along the chromosome of *B. subtilis* suggested that the translocation directionality of SpoIII<sub>C</sub>-SK could be guided by KOPS *in vivo*. To test this hypothesis, we constructed strains lacking wild-type *spoIIIIE*, but expressing either SpoIII<sup>★</sup>, SpoIII<sup>★</sup>-Δγ or SpoIII<sup>★</sup>-SK from the *spoIIIIE* promoter (Supplementary Methods) and examined their ability to translocate DNA directionally *in vivo* by measuring the number of viable spores per ml produced by each strain and the ability of SpoIII<sup>★</sup>-SK to translocate DNA directionally. Notably, we found that SpoIII<sup>★</sup>-SK rescued sporulation to near wild-type levels (Fig. 4d) and translocated DNA *in vivo* at wild-type velocities (data not shown). In contrast to SpoIII<sup>★</sup>-Δγ, less than 3% of SpoIII<sup>★</sup>-SK cells showed reversals of DNA translocation direction ( $n = 72$ , Fig. 4e), and the remaining 97% completed DNA translocation into the forespore. These experiments reveal that the γ-domains of the FtsK/SpoIIIIE family of DNA translocases are functional modules that seem to have evolved for the recognition of specific DNA sequences and can be interchanged between motors to confer different sequence-recognition properties.

### SpoIIIIE-γ regulates the compartmental localization of SpoIIIIE

So far, our data suggest that directional DNA transfer during sporulation is regulated by orientation-specific interactions between SpoIIIIE and highly skewed chromosomal sequences that switch orientation at *dif*, and not only due to the compartment-specific assembly of SpoIIIIE, as proposed by the simple exporter model. The long pauses required for reversing translocation direction *in vivo* (~20 min), however, are inconsistent with a strictly sequence-directed model (Fig. 1b) and suggest that the translocation reversal mechanism possibly involves the assembly of a forespore-specific SpoIIIIE complex. To further discern between these two models, we studied the role of SpoIIIIE-γ in compartment-specific SpoIIIIE assembly. The simple exporter model predicts that, in either the presence or the absence of SpoIIIIE-γ, SpoIIIIE should assemble a complex only in the mother cell. In contrast, the sequence-directed model suggests that SpoIIIIE may assemble on both sides of the sporulation septum.

Previous methods used to localize SpoIIIIE complexes *in vivo*, such as GFP-fusion localization, cannot distinguish SpoIIIIE localization on one side of the septum from localization on the other<sup>21</sup>. Here we used a cell-specific GFP-tagging method to visualize SpoIIIIE complexes assembled at the mother-cell or forespore side of the sporulation septum<sup>23</sup>. In this method, the leucine zipper domains of Jun and Fos (Jun<sup>LZ</sup> and Fos<sup>LZ</sup>)<sup>35</sup> are used as specific tags to link SpoIIIIE and GFP. GFP-Fos<sup>LZ</sup> was expressed in either the forespore or mother-cell compartments after septation. SpoIIIIE-Jun<sup>LZ</sup> complexes that assemble in the compartment expressing GFP-Fos<sup>LZ</sup> were visualized by the appearance of a septal GFP focus due to the binding of GFP-Fos<sup>LZ</sup> molecules to the SpoIIIIE-Jun<sup>LZ</sup> complex (Fig. 5a, right). SpoIIIIE<sup>★</sup>-Jun<sup>LZ</sup> and SpoIIIIE<sup>★</sup>-Δγ-Jun<sup>LZ</sup> were expressed from the native SpoIIIIE promoter and locus, and the frequency of focus formation in either forespore or mother-cell compartments was measured during sporulation. SpoIIIIE<sup>★</sup>-Jun<sup>LZ</sup> strains produced foci exclusively in the mother cell, as 48% of cells contained a visible mother-cell GFP focus (Fig. 5a, above,  $n = 191$ ) and 0% of cells produced forespore foci ( $n = 182$ ). In contrast, SpoIIIIE<sup>★</sup>-Δγ-Jun<sup>LZ</sup> strains produced GFP foci with approximately equal frequency in both mother-cell (53%,  $n = 210$ ) and forespore compartments (47%, Fig. 5b,  $n = 232$ ). Thus, these results conflict with both the simple exporter and the strictly sequence-directed models. In the next section, we will present a unified model for the mechanism of directional DNA transfer by SpoIIIIE/FtsK that is consistent with the available data.

## DISCUSSION

Here we advance a sequence-directed DNA exporter model for SpoIIIIE translocation directionality that is consistent with both our data and previous experiments. Structural and fluorescence microscopy evidence suggests that during sporulation each chromosome arm is translocated through an independent SpoIIIIE channel<sup>17,23,36</sup>. Our compartment-specific SpoIIIIE-tagging experiments showed that during sporulation SpoIIIIE is exclusively assembled on the mother-cell side of the septum, whereas SpoIIIIE- $\Delta\gamma$  is assembled on both sides with equal frequency. Furthermore, our fluorescence microscopy results demonstrated that SpoIIIIE- $\Delta\gamma$  can translocate DNA in both forward and reverse directions *in vivo*. These results are consistent with a model in which each chromosome arm can be initially translocated by opposing unidirectional complexes, one on each side of the newly formed division septum (forespore and mother-cell exporters, Fig. 6a). Our study reveals that SpoIIIIE- $\gamma$  not only mediates orientation-specific SpoIIIIE-SRS interactions *in vitro*, but is also required for the disassembly of the forespore exporter and the maintenance of persistent directional DNA transfer *in vivo*. The long pause durations required for reversing translocation direction by SpoIIIIE- $\Delta\gamma$  in our *in vivo* DNA translocation assay (~20 min) further suggest that the mechanism giving rise to translocation reversals is slow and may involve the reassembly of the forespore complex. Recent studies determined that the ability of SpoIIIIE to hydrolyze ATP is required for the disassembly of the forespore SpoIIIIE complex and that the orientation of the chromosome after septation determines the direction of DNA translocation<sup>23</sup>. Taken together, these results suggest that translocation by the forespore exporter leads to specific interactions between SpoIIIIE- $\gamma$  and nonpermissive SRS that lead to the inactivation and subsequent dissociation of the forespore complex (Fig. 6b,c), a process that ultimately decides the direction of DNA transfer. This model explains the observation that SpoIIIIE expressed in the forespore after septation is severely deficient in DNA export into the mother cell<sup>21</sup>, as the forespore complex may be frequently disassembled by interactions with nonpermissive SRS. The idea that SpoIIIIE may not be required on the forespore side of the septum for forward translocation from the mother cell is supported by two observations: (i) the expression of SpoIIIIE only in the mother cell after septation was shown to rescue viable spore production to near wild-type levels<sup>21</sup>; and (ii) highly homologous motors of the SpoIIIIE/FtsK family involved in conjugative transfer (such as the Tra protein from pIJ101 in *Streptomyces lividans*<sup>37</sup>) are present only in the donor-cell side of the communicating cell wall. Thus, compartment-specific localization may be relevant to the mechanisms for directional DNA transfer during cell division, sporulation and conjugation.

Previous studies proposed that the oriented loading of FtsK on KOPS<sup>29</sup>, or the reversal of translocation direction of FtsK upon encountering nonpermissive KOPS<sup>19,29,38</sup> or both could act as the mechanism for setting the direction of DNA translocation. The ability of SpoIIIIE to translocate DNA substrates lacking SRS (Supplementary Fig. 5a), the interaction of SpoIIIIE with nonpermissive SRS repeats distant from the SpoIIIIE initiation site, the requirement for the ATPase activity of SpoIIIIE to disassemble the forespore complex<sup>23</sup>, and the low density of SRS and KOPS along the chromosome suggest these sequences are not simply loading sites for SpoIIIIE/FtsK *in vivo*. The detailed molecular mechanism by which SpoIIIIE- $\gamma$ -SRS and FtsK- $\gamma$ -KOPS interactions specifically affect translocation directionality and the process by which *in vitro* reversibility is related to the mechanism of SpoIIIIE/FtsK *in vivo* remain unclear and will be the subject of our future studies.

Our sequence-directed DNA exporter model predicts that, in the absence of SpoIIIIE- $\gamma$ , the initial direction of DNA translocation early in sporulation would partition between forward and reverse orientations with equal probabilities. However, quantitative analysis of our live time-lapse microscopy data showed that SpoIIIIE- $\Delta\gamma$  commences translocation predominantly in the forward direction (>96%,  $n = 32$ ). These results imply the existence of additional

mechanisms that bias the initial direction of DNA segregation. Several possible DNA sequence-independent processes could contribute to the initial inactivation of the forespore exporter and thus produce the observed bias of the initial DNA translocation direction. The frequent reverse translocations by SpoIIIE in *minCD*-null strains<sup>22</sup> suggest that MinCD may influence chromosome architecture or inactivate forespore SpoIIIE complexes. Alternative mechanisms may involve forespore-specific DNA-protein complexes that could obstruct DNA translocation by the forespore SpoIIIE exporter by creating DNA roadblocks or membrane anchors. These complexes could include the ParB homolog Spo0J, which compacts the origin-proximal region into filamentous protein-DNA architectures<sup>1,39,40</sup>, and RacA, which tightly tethers the chromosomal origin to the cell pole<sup>40-42</sup>. The late appearance of translocation reversal events could be related to the release of *oriC* tethering later in the process of sporulation. Finally, other unknown forespore-specific factors, asymmetric concentrations of SpoIIIE between compartments or early structural asymmetry in the sporulation septum may bias the activation state of the forespore exporter at the onset of DNA translocation.

Despite these possible overlapping mechanisms, our data demonstrate that DNA sequence recognition is both robust and necessary for directional DNA translocation by SpoIIIE. Our model for sequence-directed DNA export may also explain the directional chromosomal transfer by FtsK and SpoIIIE during vegetative growth, as DNA sequence asymmetry alone could bias the activation state of exporter complexes in the absence of compartmental asymmetry. Overall, the data presented here reconcile previous contradictory models for FtsK and SpoIIIE, and suggest a new sequence-directed DNA exporter model for the establishment of translocation polarity of the FtsK/SpoIIIE/Tra family of DNA transporters.

## METHODS

### SpoIIIE<sub>C</sub> cloning and purification

SpoIIIE expression constructs were derived from pJB103 (ref. 7), which contains the C-terminal motor domain of SpoIIIE with an N-terminal OmpA tag and a C-terminal hexahistidine tag (plasmid provided by J. Bath, Oxford University). PredictProtein<sup>43</sup> was used to create a multiple sequence alignment and to predict conserved regions, secondary structure and unstructured regions. Point mutations were introduced using the QuickChange Method (Stratagene). All clones were propagated in *E. coli* DH5a cells and verified by sequencing. For further details see Supplementary Methods. SpoIIIE<sub>C</sub> was expressed and purified as described<sup>7</sup>. Pure fractions (>95% pure by SDS-PAGE and Coomassie blue staining) were pooled, dialyzed in storage buffer (50 mM HEPES, 100 mM NaCl, 0.1 mM EDTA, 30% (v/v) glycerol, pH 7.5) and quantified using optical density and the Bradford method.

### Triplex displacement assays

Fluorescent triplex substrates were designed as described in Levy *et al.*<sup>19</sup> and prepared following the method developed by McClelland *et al.*<sup>44</sup>. Displacement reactions were conducted at 25 °C in 50 mM Tris (pH 7.5), 5 mM MgCl<sub>2</sub>, 3 mM ATP, 0.1 mg ml<sup>-1</sup> BSA, 10 nM 5'-6-rhodamine triplex substrate and 20–50 nM SpoIIIE or 100nM SpoIIIE-SK chimera. Reactions were quenched by the addition of an equal volume of 250 mM MES (pH 5.5), 3% (w/v) SDS, 15% (w/v) glucose<sup>45</sup> and analyzed on 1.5% agarose gels (40 mM Tris acetate (pH 5.5), 5 mM sodium acetate, 1 mM MgCl<sub>2</sub> at 10 V cm<sup>-1</sup> at 4 °C<sup>8</sup>). Results were visualized using Typhoon Imager and the proportion of free oligonucleotide to triplex substrate was determined by using IMAGEQUANT (GE Healthcare). The percentage of free triplex at zero time was subtracted from each time point, and the percentage of triplex displaced versus time was fitted to  $A_0(1 - e^{-kt})$ , where the rate ( $k$ ) and the baseline ( $A_0$ ) were floated. Further details can be found in the Supplementary Methods.



### Magnetic tweezers experiments

DNA tethers were prepared as previously described<sup>27</sup>, using a plasmid containing a 12.2-kb segment of the *E. coli* genome devoid of any FRS or KOPS family motifs<sup>18,19</sup>. SRS repeats were synthesized as 5'-phosphorylated duplex oligonucleotides and cloned into the desired location (Supplementary Methods). To create DNA tethers, the plasmid described above was digested with XbaI and KpnI to create inserts of 12.2 kb with the SRS repeat located 3 kb from the KpnI end. These molecules were ligated to biotin- and digoxigenin-modified PCR products. DNA tethers were oriented between a biotin-BSA-straptavidin-coated glass surface and a 1- $\mu$ m diameter anti-digoxigenin antibody coated bead (DynaI, My One Beads). Tweezers experiments were conducted on a magnetic tweezers instrument described<sup>46</sup>. SpoIIIIE reactions contained: 1–3 nM SpoIIIIE<sub>C</sub>, 50 mM Tris-HCl (pH 7.5), 3mM ATP, 1–3 nM SpoIIIIE and 0.1 mg ml<sup>-1</sup> BSA at constant forces between 5–8 pN. See Supplementary Methods for additional information.

### Spore titer assay and sporulation time-lapse microscopy

Spore titers were determined as described<sup>47</sup>. Briefly, strains were inoculated into Difco sporulation medium and incubated at 37 °C and 2,600 × g for 24 h. Cultures were heated to 80 °C for 10 min, diluted in 1× TBase and plated onto LB agar plates for determining colony numbers. Time-lapse microscopy experiments were performed as described<sup>23</sup>. Briefly, exponentially growing cultures were induced to sporulate by resuspension<sup>48</sup> at 30 °C and grown for a further 2 h in the presence of 0.5  $\mu$ g ml<sup>-1</sup> FM4-64 (Molecular Probes/Invitrogen) and 0.5  $\mu$ M SytoxGreen (Invitrogen). Sporulation supernatants were collected and an additional 0.5  $\mu$ g ml<sup>-1</sup> of FM4-64 was added. Molten agarose was added to 1% final, poured into shallow-welled microscope slides (VWR; 18 mm × 1.75 mm), and allowed to solidify. Cultures were applied to the agarose pads and imaged at 30 °C using an Applied Precision Spectris microscope with a WeatherStation temperature control chamber. Exposure times varied between 100 ms and 300 ms with neutral density filter settings of 32% for both FM4-64 and SytoxGreen images. Image files were deconvolved using SoftWoRx (15 iterations on conservative setting). The 'polygon' function of ImageJ software (<http://rsb.info.nih.gov/ij/>) was used to quantitate forespore and mother-cell fluorescence signals.

### SRS *in vivo* recognition experiments

Strains were grown in DSM medium<sup>47</sup> + 1.5  $\mu$ g ml<sup>-1</sup> kanamycin at 37 °C for 24 h, heat killed for 20 min at 80 °C, diluted in 1× TBase<sup>47</sup> and plated onto LB and LB + 15  $\mu$ g ml<sup>-1</sup> kanamycin plates. Strains containing the *tet* gene in both orientations produced no measurable difference in kanamycin sensitive spore frequency (data not shown). Further details can be found in Supplementary Methods.

### Cell-specific GFP tagging

Cell-specific Jun<sup>LZ</sup>- and Fos<sup>LZ</sup>-tagging experiments were performed as described<sup>23</sup>. Briefly, exponentially growing cultures were induced to sporulate in the presence of 0.5  $\mu$ g ml<sup>-1</sup> FM4-64 (Invitrogen). Cultures were adjusted to 0.2  $\mu$ g ml<sup>-1</sup> SYTOX Green dye, applied to poly-L-lysine-coated coverslips and imaged using an Applied Precision microscope. Images were deconvolved using SoftWoRx v3.3.6 (Applied Precision).

### Strain construction, cloning *in vivo* constructs and culture conditions

All strains (Supplementary Table 2) are derived from *B. subtilis* PY79 and were created using standard methods<sup>49</sup>. Sporulation was induced by resuspension<sup>48</sup> at 30 °C. Strains, cloning and construct design details can be found in Supplementary Methods.

## Supplementary Material

Refer to Web version on PubMed Central for supplementary material.

## Acknowledgments

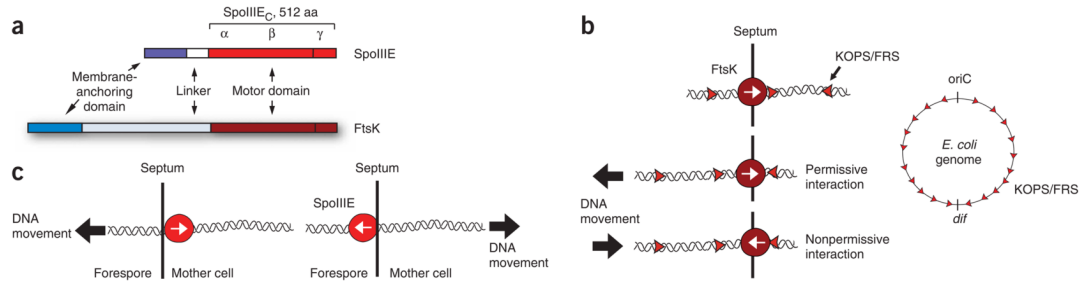
The authors would like to dedicate this work to our friend and colleague Nicholas R. Cozzarelli, who passed away during completion of this research. We thank J. Berger for his continuous advice during this research and N. Crisona for critical reading. This work was supported by National Institutes of Health Grants GM31655 (to N.R.C.) and the Human Frontier Science Program (M.N.).

## References

1. Ryter A. Morphologic study of the sporulation of *Bacillus subtilis*. *Ann Inst Pasteur (Paris)* 1965;108:40–60. [PubMed: 14289982]
2. Thomaidis HB, Freeman M, El Karoui M, Errington J. Division site selection protein DivIVA of *Bacillus subtilis* has a second distinct function in chromosome segregation during sporulation. *Genes Dev* 2001;15:1662–1673. [PubMed: 11445541]
3. Levin PA, Losick R. Transcription factor Spo0A switches the localization of the cell division protein FtsZ from a medial to a bipolar pattern in *Bacillus subtilis*. *Genes Dev* 1996;10:478–488. [PubMed: 8600030]
4. Pogliano J, Sharp MD, Pogliano K. Partitioning of chromosomal DNA during establishment of cellular asymmetry in *Bacillus subtilis*. *J Bacteriol* 2002;184:1743–1749. [PubMed: 11872726]
5. Wu LJ, Errington J. *Bacillus subtilis* spoIIIE protein required for DNA segregation during asymmetric cell division. *Science* 1994;264:572–575. [PubMed: 8160014]
6. Wu LJ, Lewis PJ, Allmansberger R, Hauser PM, Errington J. A conjugation-like mechanism for prespore chromosome partitioning during sporulation in *Bacillus subtilis*. *Genes Dev* 1995;9:1316–1326. [PubMed: 7797072]
7. Bath J, Wu LJ, Errington J, Wang JC. Role of *Bacillus subtilis* SpoIIIE in DNA transport across the mother cell-prespore division septum. *Science* 2000;290:995–997. [PubMed: 11062134]
8. Sharpe ME, Errington J. Postseptational chromosome partitioning in bacteria. *Proc Natl Acad Sci USA* 1995;92:8630–8634. [PubMed: 7567988]
9. Britton RA, Grossman AD. Synthetic lethal phenotypes caused by mutations affecting chromosome partitioning in *Bacillus subtilis*. *J Bacteriol* 1999;181:5860–5864. [PubMed: 10482533]
10. Lemon KP, Grossman AD. Effects of replication termination mutants on chromosome partitioning in *Bacillus subtilis*. *Proc Natl Acad Sci USA* 2001;98:212–217. [PubMed: 11134515]
11. Liu G, Draper GC, Donachie WD. FtsK is a bifunctional protein involved in cell division and chromosome localization in *Escherichia coli*. *Mol Microbiol* 1998;29:893–903. [PubMed: 9723927]
12. Iyer LM, Makarova KS, Koonin EV, Aravind L. Comparative genomics of the FtsK-HerA superfamily of pumping ATPases: implications for the origins of chromosome segregation, cell division and viral capsid packaging. *Nucleic Acids Res* 2004;32:5260–5279. [PubMed: 15466593]
13. Capiaux H, Lesterlin C, Perals K, Louarn JM, Cornet F. A dual role for the FtsK protein in *Escherichia coli* chromosome segregation. *EMBO Rep* 2002;3:532–536. [PubMed: 12034757]
14. Wu LJ, Errington J. Septal localization of the SpoIIIE chromosome partitioning protein in *Bacillus subtilis*. *EMBO J* 1997;16:2161–2169. [PubMed: 9155041]
15. Wang L, Lutkenhaus J. FtsK is an essential cell division protein that is localized to the septum and induced as part of the SOS response. *Mol Microbiol* 1998;29:731–740. [PubMed: 9723913]
16. Yu XC, Tran AH, Sun Q, Margolin W. Localization of cell division protein FtsK to the *Escherichia coli* septum and identification of a potential N-terminal targeting domain. *J Bacteriol* 1998;180:1296–1304. [PubMed: 9495771]
17. Massey TH, Mercogliano CP, Yates J, Sherratt DJ, Lowe J. Double-stranded DNA translocation: structure and mechanism of hexameric FtsK. *Mol Cell* 2006;23:457–469. [PubMed: 16916635]
18. Bigot S, et al. KOPS: DNA motifs that control *E. coli* chromosome segregation by orienting the FtsK translocase. *EMBO J* 2005;24:3770–3780. [PubMed: 16211009]

19. Levy O, et al. Identification of oligonucleotide sequences that direct the movement of the *Escherichia coli* FtsK translocase. *Proc Natl Acad Sci USA* 2005;102:17618–17623. [PubMed: 16301526]
20. Pease PJ, et al. Sequence-directed DNA translocation by purified FtsK. *Science* 2005;307:586–590. [PubMed: 15681387]
21. Sharp MD, Pogliano K. Role of cell-specific SpoIIIE assembly in polarity of DNA transfer. *Science* 2002;295:137–139. [PubMed: 11778051]
22. Sharp MD, Pogliano K. MinCD-dependent regulation of the polarity of SpoIIIE assembly and DNA transfer. *EMBO J* 2002;21:6267–6274. [PubMed: 12426398]
23. Becker EC, Pogliano K. Cell-specific SpoIIIE assembly and DNA translocation polarity are dictated by chromosome orientation. *Mol Microbiol* 2007;66:1066–1079. [PubMed: 18001347]
24. Partridge SR, Errington J. The importance of morphological events and intercellular interactions in the regulation of prespore-specific gene expression during sporulation in *Bacillus subtilis*. *Mol Microbiol* 1993;8:945–955. [PubMed: 8355618]
25. Lewis PJ, Partridge SR, Errington J. Sigma factors, asymmetry, and the determination of cell fate in *Bacillus subtilis*. *Proc Natl Acad Sci USA* 1994;91:3849–3853. [PubMed: 8171000]
26. Pogliano J, et al. A vital stain for studying membrane dynamics in bacteria: a novel mechanism controlling septation during *Bacillus subtilis* sporulation. *Mol Microbiol* 1999;31:1149–1159. [PubMed: 10096082]
27. Ptacin JL, Nollmann M, Bustamante C, Cozzarelli NR. Identification of the FtsK sequence-recognition domain. *Nat Struct Mol Biol* 2006;13:1023–1025. [PubMed: 17041598]
28. Sivanathan V, et al. The FtsK  $\gamma$  domain directs oriented DNA translocation by interacting with KOPS. *Nat Struct Mol Biol* 2006;13:965–972. [PubMed: 17057717]
29. Bigot S, Saleh OA, Cornet F, Allemand JF, Barre FX. Oriented loading of FtsK on KOPS. *Nat Struct Mol Biol* 2006;13:1026–1028. [PubMed: 17041597]
30. Griffiths AA, Wake RG. Search for additional replication terminators in the *Bacillus subtilis* 168 chromosome. *J Bacteriol* 1997;179:3358–3361. [PubMed: 9150236]
31. Sciochetti SA, Piggot PJ, Blakely GW. Identification and characterization of the *dif* site from *Bacillus subtilis*. *J Bacteriol* 2001;183:1058–1068. [PubMed: 11208805]
32. Becker E, et al. DNA segregation by the bacterial actin AlfA during *Bacillus subtilis* growth and development. *EMBO J* 2006;25:5919–5931. [PubMed: 17139259]
33. Hendrickson H, Lawrence JG. Selection for chromosome architecture in bacteria. *J Mol Evol* 2006;62:615–629. [PubMed: 16612541]
34. Wu LJ, Errington J. A large dispersed chromosomal region required for chromosome segregation in sporulating cells of *Bacillus subtilis*. *EMBO J* 2002;21:4001–4011. [PubMed: 12145201]
35. Kohler JJ, Schepartz A. Kinetic studies of FosJunDNA complex formation: DNA binding prior to dimerization. *Biochemistry* 2001;40:130–142. [PubMed: 11141063]
36. Burton BM, Marquis KA, Sullivan NL, Rapoport TA, Rudner DZ. The ATPase SpoIIIE transports DNA across fused septal membranes during sporulation in *Bacillus subtilis*. *Cell* 2007;131:1301–1312. [PubMed: 18160039]
37. Pettis GS, Cohen SN. Unraveling the essential role in conjugation of the Tra protein of *Streptomyces lividans* plasmid pIJ101. *Antonie Van Leeuwenhoek* 2001;79:247–250. [PubMed: 11816966]
38. Bigot S, Sivanathan V, Possoz C, Barre FX, Cornet F. FtsK, a literate chromosome segregation machine. *Mol Microbiol* 2007;64:1434–1441. [PubMed: 17511809]
39. Sharpe ME, Errington J. The *Bacillus subtilis* *soj-spo0J* locus is required for a centromere-like function involved in prespore chromosome partitioning. *Mol Microbiol* 1996;21:501–509. [PubMed: 8866474]
40. Wu LJ, Errington J. RacA and the Soj-Spo0J system combine to effect polar chromosome segregation in sporulating *Bacillus subtilis*. *Mol Microbiol* 2003;49:1463–1475. [PubMed: 12950914]
41. Ben-Yehuda S, Rudner DZ, Losick R. RacA, a bacterial protein that anchors chromosomes to the cell poles. *Science* 2003;299:532–536. [PubMed: 12493822]
42. Ben-Yehuda S, et al. Defining a centromere-like element in *Bacillus subtilis* by identifying the binding sites for the chromosome-anchoring protein RacA. *Mol Cell* 2005;17:773–782. [PubMed: 15780934]

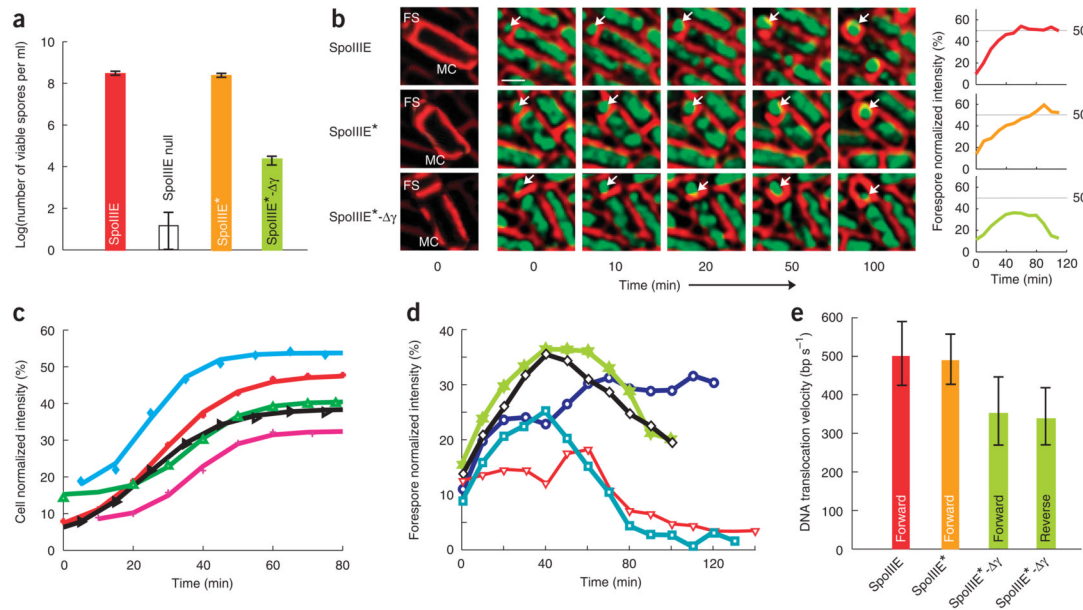
43. Rost B, Yachdav G, Liu J. The PredictProtein server. *Nucleic Acids Res* 2004;32:W321–W326. [PubMed: 15215403]
44. McClelland SE, Dryden DT, Szczelkun MD. Continuous assays for DNA translocation using fluorescent triplex dissociation: application to type I restriction endonucleases. *J Mol Biol* 2005;348:895–915. [PubMed: 15843021]
45. Firman K, Szczelkun MD. Measuring motion on DNA by the type I restriction endonuclease EcoR124I using triplex displacement. *EMBO J* 2000;19:2094–2102. [PubMed: 10790375]
46. Strick TR, Allemand JF, Bensimon D, Croquette V. Behavior of supercoiled DNA. *Biophys J* 1998;74:2016–2028. [PubMed: 9545060]
47. Perez AR, Abanes-De Mello A, Pogliano K. SpoIIB localizes to active sites of septal biogenesis and spatially regulates septal thinning during engulfment in *Bacillus subtilis*. *J Bacteriol* 2000;182:1096–1108. [PubMed: 10648537]
48. Sterlini JM, Mandelstam J. Commitment to sporulation in *Bacillus subtilis* and its relationship to development of actinomycin resistance. *Biochem J* 1969;113:29–37. [PubMed: 4185146]
49. Hoch JA. Genetic analysis in *Bacillus subtilis*. *Methods Enzymol* 1991;204:305–320. [PubMed: 1943780]



**Figure 1.**

Architecture of SpoIIIE and FtsK monomers and models for DNA translocation directionality. **(a)** Schematic depicting the architecture of the SpoIIIE and FtsK monomers (above and below, respectively), showing the N-terminal transmembrane domain (blue), the central linker domain (white) and the motor domain consisting of  $\alpha$ ,  $\beta$  and  $\gamma$  subdomains (red). **(b)** Sequence-directed model for DNA translocation directionality of FtsK. Above left, FtsK moves along DNA in the direction of the white arrow. The encounter of FtsK with KOPS in the permissive direction (rightward-pointing red arrowheads) does not affect the translocation direction (middle left). FtsK can reverse translocation direction (below left) when encountering KOPS in the nonpermissive orientation (leftward-pointing red arrowheads). KOPS are highly skewed in the chromosome of *E. coli* and switch strand and orientation at *dif* (right). **(c)** Simple exporter model for DNA translocation directionality by SpoIIIE. In this model, the relative abundance of SpoIIIE (red circle, arrows indicating its relative orientation) in the mother cell or other cell-specific factors favor the assembly of a unidirectional DNA exporter in the mother cell that determines the directionality of transfer (left). Expression of SpoIIIE in the forespore after septation leads to DNA transfer into the mother cell<sup>21</sup> (right).



**Figure 2.**

SpoIIIIE- $\gamma$  is necessary for efficient sporulation but does not affect motor function. **(a)** Log of viable spore titers for wild-type (red), SpoIIIIE null (white), SpoIIIIE\* (orange) and SpoIIIIE\* $\Delta\gamma$  (green) cells. Error bars indicate s.d. **(b)** Timelapse microscopic images of wild-type (above), SpoIIIIE\* (middle) and SpoIIIIE\* $\Delta\gamma$  (below) cells. Membrane images (red) at the left are enhanced to indicate the location and orientation of the cell in each frame, and the forespore and mother cell are indicated (FS and MC, respectively). A time-lapse image series is shown, with arrows indicating the forespore DNA (green). The scale bar of 1  $\mu\text{m}$  is shown. Plots to the right of each series show the normalized forespore intensity versus time. **(c)** Normalized DNA fluorescence intensity in the forespore versus that in the mother cell from time-lapse fluorescence images of SpoIIIIE\* strains permits quantification of the percentage of DNA translocated into the forespore as a function of time. **(d)** Normalized DNA fluorescence intensity traces of individual cells (different colors shown) of the SpoIIIIE\* $\Delta\gamma$  strain. **(e)** *In vivo* velocities of DNA translocation for SpoIIIIE (red), SpoIIIIE\* (orange) and SpoIIIIE\* $\Delta\gamma$  (green) obtained from DNA fluorescence intensity traces. Error bars indicate s.d.

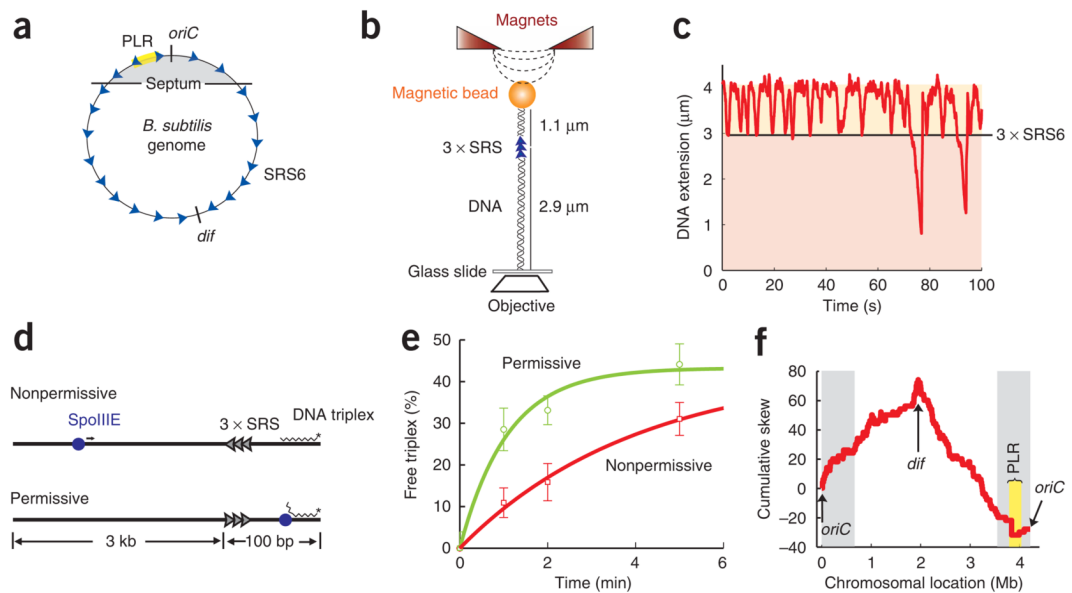


**Figure 3.**

Identification and characterization of a SpoIIIE recognition sequence (SRS). **(a)** Schematic depicting the orientation of SRS6 sequences (blue arrowheads) along the *B. subtilis* chromosome (circle). The replication origin (*oriC*), the *dif* sequence and the polar localization region (PLR) are indicated. Gray area marks the region of the chromosome initially trapped by the septum before DNA translocation by SpoIIIE commences. **(b)** Schematic depicting the magnetic tweezers setup for DNA sequence recognition. A naked double-stranded DNA molecule (black helix) is tethered between a glass slide and magnetic particle. A repeat of three SRS candidates to be tested (blue arrowheads) is located near the top, 1.1  $\mu\text{m}$  from the bead and 2.9  $\mu\text{m}$  from the glass surface. Tension in the DNA is introduced using magnets (red triangles). SpoIIIE<sub>C</sub>-induced DNA looping shortens the DNA extension, monitored by the change in height of the magnetic particle using an inverted objective (white rhombus). Specific interactions between SpoIIIE<sub>C</sub> and SRS are observed as pauses and translocation reversals at extensions corresponding to the location of the tandem repeat of three SRS sequences (3  $\times$  SRS). **(c)** Representative trace of the change in DNA extension due to single-molecule SpoIIIE<sub>C</sub> activity on a DNA molecule containing a 3  $\times$  SRS6 at the test location (black line). **(d)** Schematic of DNA triplex displacement assay. SRS repeats (arrowheads) in the nonpermissive or the permissive orientations are located on a linear duplex DNA between a 21-bp triplex (jagged line) and a 3-kb ‘antenna’ region. SpoIIIE (blue sphere) often binds within the antenna region because of its relative length. Translocation of SpoIIIE into the nonpermissive SRS region frequently reverses SpoIIIE, protecting the triplex (above). SpoIIIE translocation into the permissive SRS region leads to displacement of the triplex (below). **(e)** SpoIIIE<sub>C</sub> triplex displacement reactions on DNA substrates with permissive (green circles) or nonpermissive (red squares) SRS6 orientations. The percentage of free triplex is plotted as a function of time, and error bars indicate s.d. Data were normalized for the initial percentage of free triplex and fit to an exponential function. The ratio of displacement on nonpermissive versus permissive substrates is  $2.5 \pm 0.5$ . **(f)** Step plot indicating the locations and orientations of SRS6 along the *B. subtilis* genome (see text). Cumulative skew is shown as a function of chromosomal location (Supplementary Methods). The replication origin (*oriC*), the *dif* site and the PLR are indicated. Gray area marks the region of the chromosome initially trapped by the septum before DNA segregation by SpoIIIE commences.

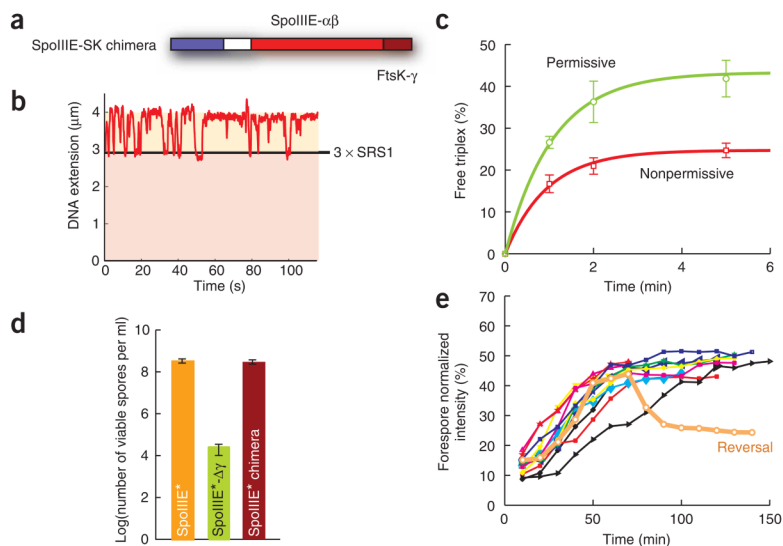


**Figure 4.**  $\gamma$ -domains are modular and can be switched between species to confer altered DNA sequence specificities. **(a)** Schematic depicting the architecture of the SpoIIIE-SK chimera containing the  $\gamma$ -domain of FtsK (dark red) fused to the motor domain of SpoIIIE (light red). **(b)** Representative trace of SpoIIIE<sub>C</sub>-SK chimera-induced changes in DNA extension versus time in the magnetic tweezers on a DNA substrate containing a triple repeat of KOPS ( $3 \times \text{SRS1}$ ) at the test location (black line). **(c)** SpoIIIE<sub>C</sub>-SK chimera DNA triplex displacement reactions on substrates containing either a triple KOPS sequence in permissive (green circles) or nonpermissive (red squares) orientations. Error bars indicate s.d. Data were normalized for the initial percentage of free triplex and fit to an exponential function. Ratio of displacement on permissive versus nonpermissive substrates is  $1.8 \pm 0.25$ . **(d)** Log of heat-resistant spore titers for wild-type SpoIIIE\* (orange), SpoIIIE\*- $\Delta\gamma$  (green) and SpoIIIE\*-SK chimera (red) strains. Error bars indicate s.d. **(e)** Normalized DNA fluorescence intensity traces of individual SpoIIIE\*-SK cells (different colors shown). Velocities of DNA translocation *in vivo* were  $520 \pm 100 \text{ bp s}^{-1}$  ( $n = 16$ ), similar to those of SpoIIIE\*.

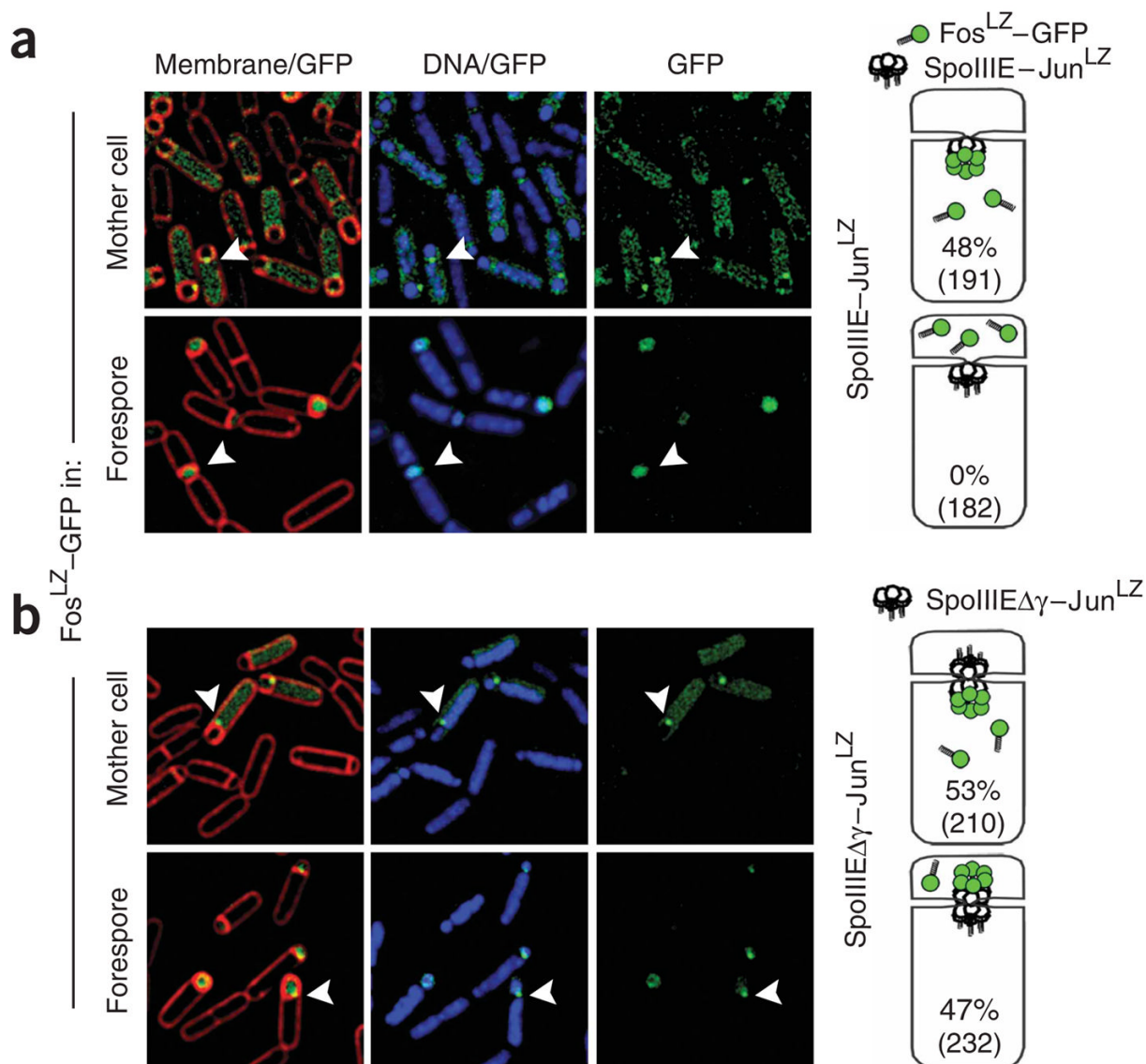


**Figure 5.** Cell-specific GFP tagging indicates that SpoIIIE- $\Delta\gamma$  assembles on both sides of the sporulation septum with equal frequency. Cartoons show the experimental setup (right). Fos<sup>LZ</sup>-GFP (green circles) was expressed after septation in the forespore or mother-cell compartments in strains expressing SpoIIIE-Jun<sup>LZ</sup> or SpoIIIE- $\Delta\gamma$ -Jun<sup>LZ</sup> (white circles). The location of SpoIIIE complexes was observed by the appearance of a GFP focus (green cluster) at the septal midpoint. Fluorescence microscopic images show a membrane and GFP overlay (left), a DNA and GFP overlay (center) and GFP only (right). GFP foci are indicated by white arrowheads. **(a)** SpoIIIE assembles only on the mother-cell side of the septum during DNA translocation. SpoIIIE-Jun<sup>LZ</sup> foci were observed on the mother-cell side of the septum in 48% of the cells ( $n = 191$ , above), whereas no SpoIIIE-Jun<sup>LZ</sup> foci were observed in the forespore compartment ( $n = 182$ , below). **(b)** SpoIIIE- $\Delta\gamma$  assembles on both sides of the septal membrane with equal frequency. Assembly of SpoIIIE- $\Delta\gamma$ -Jun<sup>LZ</sup> foci was observed in the mother cell (53%,  $n = 210$ , above) and forespore (47%,  $n = 232$ , below) sides of the septum.

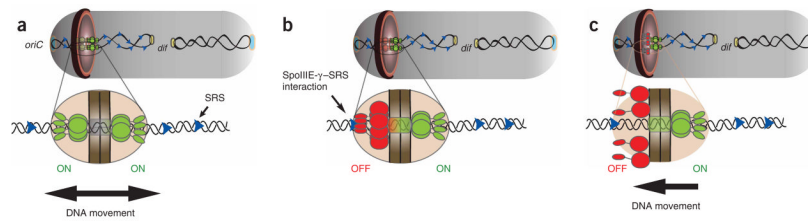


**Figure 6.**

Model for SpoIIIE sequence-directed DNA export during sporulation. **(a)** Schematic of a sporulating *B. subtilis* cell (gray) at the onset of DNA translocation, in which each chromosomal arm (black ribbon) is bound by two opposing active unidirectional complexes (green) that assemble on each side of the division septum (brown disc). Below, an enlarged view of a single chromosomal arm (helix), division septum (gray) and SRS sequences (blue triangles) are represented. Black arrows depict the overall direction of DNA transport. We assume that during translocation DNA is transported in the direction from SpoIIIE- $\beta$  to SpoIIIE- $\alpha^{29}$ ; **(b)** SpoIIIE- $\gamma$ -mediated interactions with nonpermissive SRS in the forespore leads to the inactivation of the forespore complex (red). **(c)** The inactivation of the forespore SpoIIIE complex converts the bidirectional channel into a DNA exporter, leading to unidirectional DNA transport into the forespore.